Journal Name

Supporting Information

Silica nano-channel induced i-motif formation and stabilization at neutral and alkaline pH

Sagar Satpathi, Konoya Das and Partha Hazra*[a, b]

Received 00th January 20xx,
Accepted 00th January 20xx

DOI: 10.1039/x0xx00000x
www.rsc.org/

[a] Department of Chemistry, Indian Institute of Science Education and Research (IISER), Pune. Dr. Homi Bhabha Road, Pashan, Pune, India 411008. Tel: +91-20-2590-8077. p.hazra@iiserpune.ac.in
[b] Centre for Energy Science, Indian Institute of Science Education and Research (IISER), Pune (411008), Maharashtra, India

Table S1. Different cytosine rich DNA sequences used in this study.

DNA	Sequences (5´→ 3´)
h-teloc	d(CCCTAACCCTAACCCTAACCCTAA)
TC5	d(TCCCCC)
C-Myc	d(CCCCACCTTCCCCACCCTCCCCACCCTCCCC)
bcl-2	d(CAGCCCCGCTCCCGCCCCCTTCCTCCCGCGCCCGCCCCT)
hTERT	d(CCCCGCCCCGTCCCGACCCCTCCCGGGTCCCCGGCCCAGCCCCCACCG GGCCCTCCCAGCCCCTCCCC)
2-aminopurine labelled h-teloc (Ap h-teloc)	d(CCCTApACCCTAACCCTAACCCTAA)

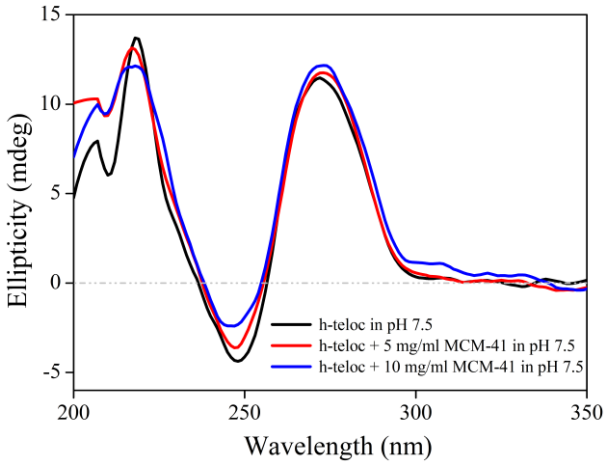

Fig. S1 Circular dichroism (CD) spectra of h-teloc in pH 7.5 buffer with increasing concentration of MCM-41.

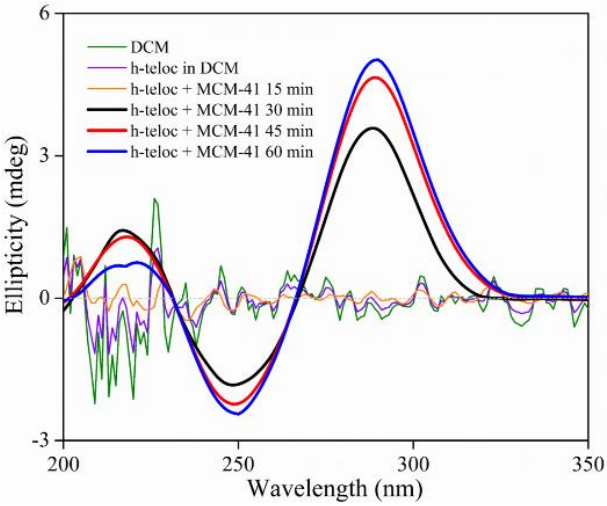

Fig. S2 Circular dichroism spectra of h-teloc in presence of MCM-41 in DCM solution with evolution of time.

Note S1- Control experiments with non i-motif forming DNA sequences:

Table S2. Different non i-motif forming DNA sequences used in this control study.

DNA	Sequences (5´→ 3´)
oligo-1	d(TTTTAATTTTAATTTTAATTTTAA)
H24	d(TTAGGGTTAGGGTTAGGGTTAGGG)

We have carried out similar experiments with other non i-motif forming DNA sequences having a same number of nucleobases (Table S2) as h-teloc (5´-CCCTAACCCTAACCCTAACCCTAA-3´) to ensure that these observations are a result of i-motif DNA formation or not. We have substituted the cytosine bases of h-teloc with thymine. Thus, this sequence (oligo-1) cannot form the i-motif DNA in any condition. We have mixed the respective DNA sequences (oligo-1 and H24) and MCM-41 in non-polar DCM solvent. Later, we have extracted the DNA loaded MCM-41 by solvent evaporation method. Then, we have dispersed the DNA loaded (oligo-1 and H24) MCM-41 in pH 7.5 buffer and deionized water. In pH 7.5 buffer, oligo-1 exhibits an ellipticity pattern with a positive peak at 279 nm and negative peak at 247 nm (Fig. S3A), whereas encapsulated oligo-1 in MCM-41 shows similar ellipticity pattern to oligo-1 with decrement in negative peak at 247 nm (Fig. S3A). This decrement in negative peak upon encapsulation may be attributed to the lesser helicity pattern arising from the confined environment inside MCM-41. Moreover, the observed ellipticity pattern for encapsulated oligo-1 in MCM-41 is distinctly different from the i-motif ellipticity pattern.

We have also performed this encapsulation with the complimentary sequence (H24) of h-teloc which is known for its G-quadruplex (GQ) formation in presence of ions, but cannot form any i-motif structure due to absence of cytosine nucleobases. In deionized water, CD spectra of H24 contains a positive peak around 260 nm and negative peak around 235 nm indicating the ssDNA/RC formation (Fig. S3B), which gets altered in presence of K^+ ion due to hybrid GQ formation exhibiting two positive peaks around 290 nm and 250 nm, and a negative peak at around 235 nm.[1] However, encapsulated H24 inside MCM-41 in deionized water as well as in presence of K^+ ion exhibits the characteristics peaks of ssDNA/RC formation with very less intensity for negative peak around 235 nm (Fig. S3B). Thus, the absence of GQ structure inside MCM-41 even in presence of K^+ ion indicates the lack of accessibility of solvent molecule or ion inside MCM-41 nano-channels. Here also, huge decrement in helicity peak (i.e. negative peak around 235 nm) upon encapsulation may be attributed to distortion of secondary structure due to the restricted environment inside MCM-41. In a nutshell, distinctly different ellipticity patterns observed for both oligo-1 and H24 loaded MCM-41 in comparison to i-motif DNA indicates that all DNA encapsulations do not lead to i-motif formation.

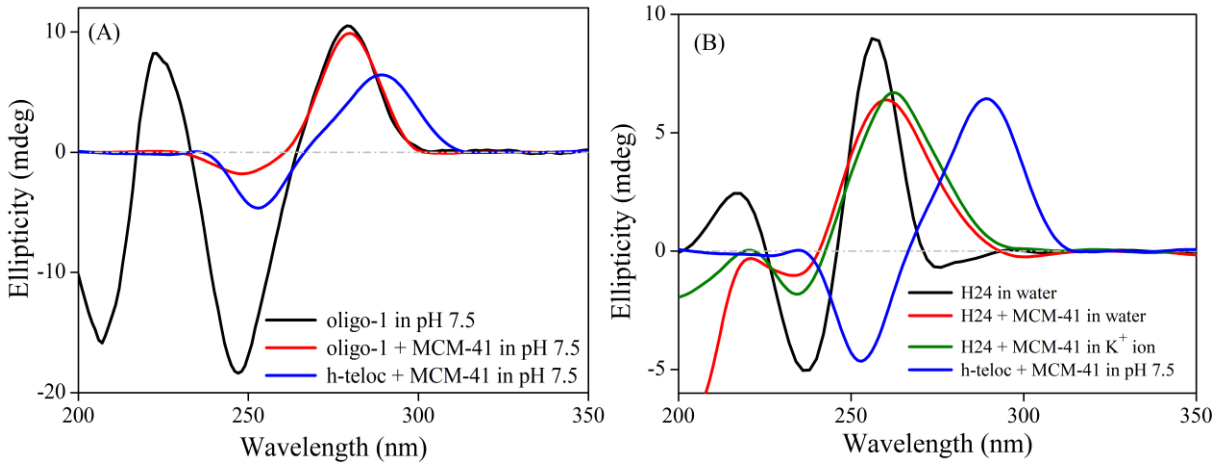

Fig. S3 Circular dichroism (CD) spectra of (A) oligo-1 and encapsulated oligo-1 inside MCM-41 in pH 7.5 buffer. (B) CD spectra of H24 and encapsulated H24 inside MCM-41 in deionised water and in K^+ ion (10 mM) containing pH 7.5 buffer.

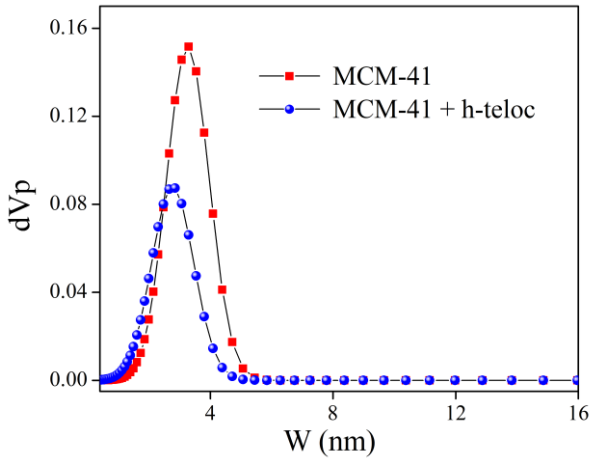

Fig. S4 Pore-size distribution of MCM-41 and MCM-41+ h-teloc system.

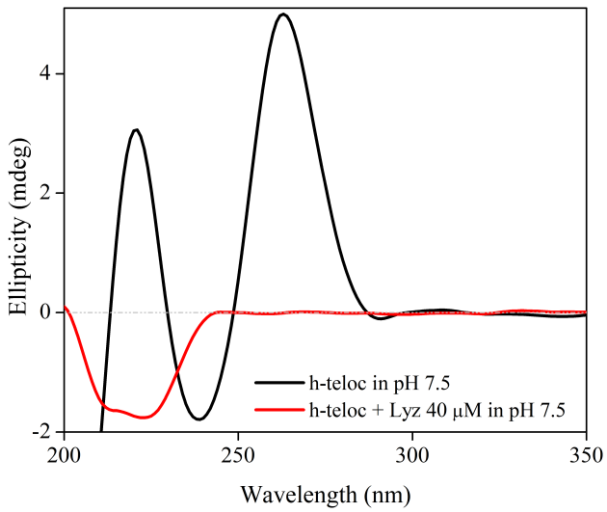

Fig. S5 Circular dichroism spectra of h-teloc in presence of Lyz protein at pH 7.5 buffer.

Note S2- Versatility of the Reversible Approach:

To check the versatility of this reversible approach, we have performed similar experiments with MCM-41 containing different C-rich sequences and Lyz (Fig. S4). Here, we have taken two other C-rich sequences, C-Myc and bcl-2 in addition to the h-teloc sequence (Table S1). CD spectra of C-Myc/bcl-2 contained in MCM-41 at pH 7.5 undergoes significant alteration in ellipticity pattern with Lyz addition. With increasing Lyz concentration, characteristic ellipticity pattern of i-motif DNA (positive peak around 290 nm and negative peak around 260 nm) decreases gradually along with the appearance of ellipticity pattern for native Lyz (negative peaks around 230 nm and 210 nm respectively). This indicates the disruption of i-motif DNA and subsequent formation of corresponding DNA and Lyz complex which is evident from their respective control experiment with C-Myc/bcl-2 and Lyz in pH 7.5 buffer (Fig. S4C).

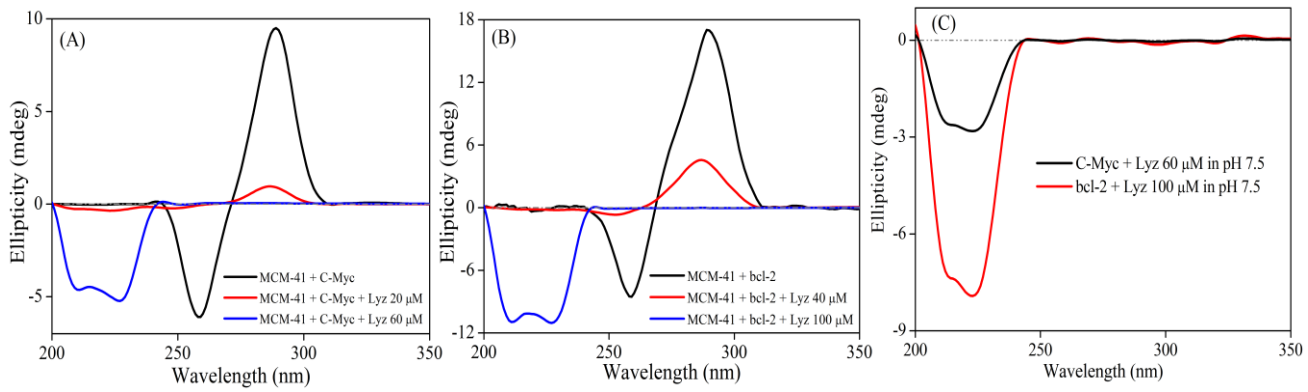

Fig. S6 CD spectra of (A) C-Myc and (B) bcl-2 encapsulated MCM-41 systems with increasing concentration of Lyz protein in pH 7.5 buffer. (C) Circular dichroism spectra of C-Myc and bcl-2 in presence of Lyz protein at pH 7.5 buffer.

Interaction of positively charged Lyz with negatively charged phosphate groups of DNAs drags the C-rich strands out of the MCM-41 nano-pores. This leads to the protein-DNA complex formation which is eventually responsible for the conformational transition from i-motif DNA to single stranded/random coil form. Another important point to mention is that higher concentration of Lyz is required for longer C-rich sequences (40 µM for h-teloc having 24 nucleobases, 60 µM for C-Myc having 31 nucleobases, 100 µM for bcl-2 having 39 nucleobases). This can be attributed to the larger number of positively charged Lyz moieties involved in the interactions with the more number of negatively charged phosphate groups present in longer C-rich sequences. This reversible approach is found to be effective for several C-rich sequences observed in different oncogenes ensuring the versatility of the approach.

Note S3- Verification of Reversible Approach in Multiple Cycles:

We have checked the reversible nature of our approach by utilizing the same MCM-41 substrate in different cycles (Fig. 3B). We have utilized the ellipticity signal at 290 nm as the indicator for i-motif structure. First, we have mixed the h-teloc and MCM-41 in non-polar DCM solvent for better encapsulation of oligo in silica nano-channels. Then, we have extracted the MCM-41 samples and repeatedly washed with buffer to remove any unbound oligo/surface bound oligo from the MCM-41. Subsequently we have dispersed this oligo loaded MCM-41 samples in pH 7.5 buffer (MCM-41+h-teloc) which shows a characteristic i-motif ellipticity pattern with a reasonable positive peak at 290 nm. Next, we have added Lyz protein in the same solution which shows the disappearance of i-motif ellipticity pattern with negligible positive peak at 290 nm (MCM-41+h-teloc+Lyz). This indicates the absence of i-motif structure in the solution. Again, we have extracted the MCM-41 samples from the solution of MCM-41+h-teloc+Lyz and washed repeatedly with buffer to remove any unbound/surface bound protein and DNA from the MCM-41. Following this, we have dispersed the extracted MCM-41 samples in DCM solvent and freshly added h-teloc in the solution. The above described processes were repeated in cycles and the ellipticity pattern was noted at each step which showed identical change as the initial cycle. This type of feasibility over several cycles may be useful in potential applications for nanotechnology.

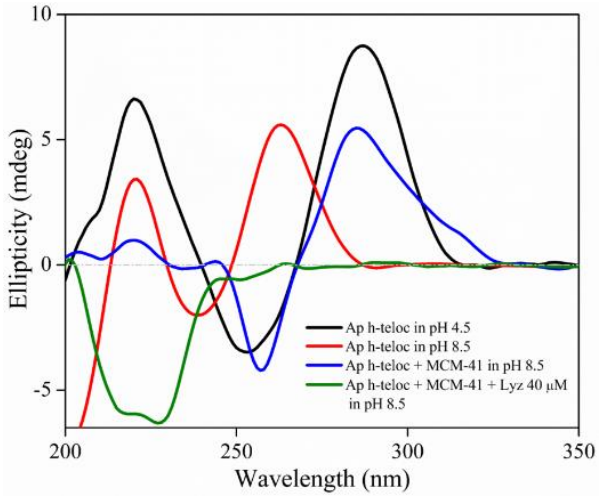

Fig. S7 Circular dichroism spectra of 2-aminopurine labelled h-teloc (Ap h-teloc) in neutral and alkaline buffer solutions. CD spectra of Ap h-teloc encapsulated MCM-41 in presence and absence of Lyz protein in pH 8.5 buffer.

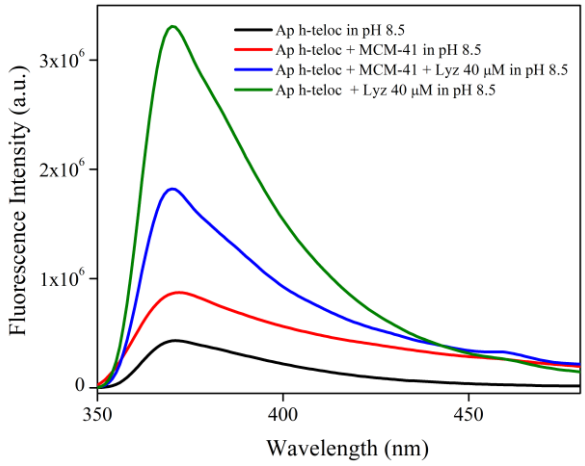

Fig. S8 Steady state fluorescence spectra of 2-aminopurine labelled h-teloc (Ap h-teloc) in presence of MCM-41 and Lyz protein in alkaline buffer solutions.

Table S3. Fluorescence transient fittings of Ap labelled h-teloc DNA in case of different systems (λ_{ex} = 285 nm and λ_{em} = 370 nm).

Sample	τ_1.(ns)	a_1	τ_1 (ns)	a_2	τ_{avg} [#, $] (ns)	χ^2
Ap h-teloc in pH 4.5	1.35	0.67	6.02	0.33	2.88	1.08
Ap h-teloc in pH 8.5	0.86	0.76	3.11	0.24	1.39	1.07
Ap h-teloc + MCM-41 in pH 8.5	0.46	0.94	3.33	0.06	0.64	1.20
Ap h-teloc + MCM-41 + Lyz 40 μM in pH 8.5	1.14	0.58	3.39	0.42	2.07	1.07
Ap h-teloc + Lyz 40 μM in pH 8.5	1.63	0.73	5.09	0.27	2.55	1.10

[#]$\tau_{avg} = a_1\tau_1 + a_2\tau_2$

[$]We have considered the average lifetime values for explanation of the results to minimize the complexity.

Materials and Methods

All the C-rich DNA sequences, oligo-1 and H24 DNA were purchased from Integrated DNA Technologies (IDT) and used as received. Mesoporous silica (MCM-41), hen egg white lysozyme (>90% purity) were purchased from Sigma-Aldrich and used without any further purification. Mesoporous silica (MCM-41) with a pore diameter of 20–30 Å is dried in a vacuum oven at 300°C in order to remove trace amount of encapsulated water molecules. Molecular biology grade Na_2HPO_4 and NaH_2PO_4 are procured from Sisco Research Laboratories (SRL India). We have performed all the experiments with 10 mM phosphate buffer solutions of different pH. Prior to the experiments, DNA samples were annealed at 90 °C for 10 min and stored at 4 °C for 24 h. Concentrations of DNA samples were determined using the molar extinction coefficient at 260 nm provided by IDT, USA. It is necessary to mention here that IDT has determined the molar extinction coefficient using nearest neighbor approximation model. The concentration of lysozyme was calculated using the molar extinction coefficient of 37970 M^{-1} cm^{-1} at 280 nm.[2] Prior to the experiments, we have prepared the samples and kept it overnight for measurements. We have used the crystal structure of Lyz (PDB ID- 254L) for the table of content preparation.[3]

Circular dichroism (CD) spectra were recorded on a J-815 CD (JASCO, U.S.A.) instrument at 25°C. The data were collected at 1 nm intervals with 1 nm band width. Each CD profile is an average of 3 scans of the same sample collected at a scan speed 100 nm/min, with a proper baseline correction from the buffer/DCM solution. The surface area, pore size and pore volume were determined by using N_2 adsorption–desorption isotherms obtained at 77 K on BelSorpmax (Bel Japan) apparatus. The purity of nitrogen used in adsorption experiments was 99.99%. Before adsorption measurements, the samples (MCM-41 and MCM-41+h-teloc) were heated at 120 °C under vacuum for 24 hours. The specific surface area and pore size distribution were obtained from the analysis of the adsorption–desorption isotherms using Brunauer–Emmett–Teller (BET) and Non-Localized Density Functional Theory (NLDFT) methods, respectively. Steady state fluorescence measurements were carried out in FluoroMax-4 spectrofluorimeter (Horiba Scientific, U.S.A.). Lifetime measurements were performed using time correlated single photon counting (TCSPC) setup (Horiba Jobin Yvon, U.S.A.). Ap labelled h-teloc samples were excited using the 285 nm nano-led (fwhm ~1 ns) and the photons at respective emission maximums at magic angle were collected using a MCP-PMT (Hamamatsu, Japan) detector. Decay profiles were analyzed using IBH DAS6 software. Decays were fitted with minimum number of exponentials based on the χ^2 values and the visual inspection of the residuals quality.

References

1. S. Satpathi, M. Kulkarni, A. Mukherjee and P. Hazra *Phys. Chem. Chem. Phys.*, 2016, **18**, 29740-29746.
2. S. Klitgaard, M. T. Neves-Petersen and S. B. Petersen, *J. Fluoresc.*, 2006, **16**, 595–609.
3. B K Shoichet, W A Baase, R Kuroki and B W Matthews, *Proc. Natl. Acad. Sci. USA*, 1995, **92**, 452-456.